A DYNAMIC RMS-MODEL OF THE LOCAL VOLTAGE CONTROL SYSTEM Q(V) APPLIED IN PHOTOVOLTAIC INVERTERS

Marco LINDNER
Institute of Power Transmission Systems
Technische Universität München - Germany
marco.lindner@tum.de

Rolf WITZMANN
Institute of Power Transmission Systems
Technische Universität München - Germany
rolf.witzmann@tum.de

ABSTRACT

The additional integration of distributed energy resources (DER) into today's electricity distribution grids is planned and anticipated in many countries. As a consequence, local voltage stability problems will be multiplied and their prevention will become crucial to the security of electricity supply. Voltage source inverters represent the largest share of grid connection solutions. Their ability of almost independent reactive power supply can be utilized to manage local voltage- and in particular local voltage rise problems in distribution grids. Of notably interest are the widely researched approaches using cosφ(P)- or Q(V)-characteristics. While the implementation of a cosφ(P)-characteristic is simply done by an open-loop structure, a control system such as Q(V) includes a feedback loop and is therefore exposed to possible unstable operation. This instability is subject to the internal control structure and parameterization of the respective inverter, which is usually not publicly accessible. Yet, knowledge of stability and dynamic performance of new technologies is essential for their broad acceptance. In this paper, two dynamic reactive power control RMS-models are developed from and evaluated with laboratory measurements.

INTRODUCTION

To assess the possible integration of new DER, loads or other electrical equipment into an electricity distribution grid, load flow simulations using basic models are initially performed. Those models are usually static or of minor dynamic validity. When it comes to the implementation of automated control structures, such as local voltage control by Q(V), the system stability can be endangered by unknown reactions to dynamic events. Parameterization of the control system's architecture allows the possibility to influence the dynamic performance of the converter. However, without any knowledge of the system's design, even apparently "safe" parameters can lead to unstable operation in specific cases. Previous works focused on theoretical stability of (simplified) local voltage control systems [1,2] and laboratory evaluations [3,4] as well as parametric studies of up-to-date photovoltaic inverters [5]. Nevertheless, a guarantee or realistic forecast of a system's stability cannot be made upon those facts, since parametric studies are based on simplified processes (grid as one transmission line) and simplified system models neglect effects of nonlinear operation and manufacturer-specific design. The lack of knowledge about the systems dynamic performance and missing regulatory specifications may explain why automated local voltage control systems are not yet implemented and activated in many electricity distribution grids. In order to gain acceptance of and insight into such control systems, the aim of this paper is to establish representative, dynamic RMS-models of two up-to-date inverters to be implemented in simulation environments and included in stability analyses.

LABORATORY ENVIRONMENT

The laboratory environment (see Figure 1) used to test the photovoltaic inverters consists of a full programmable three-phase low-voltage source, lumped transmission line elements (resistive 'R' and inductive 'X') with line parameter settings according to a 5.5km NAYY 4x150 mm^2 cable, and a measurement system with high resolution (up to 100kHz). Arbitrary voltage signals can be generated on each phase individually.

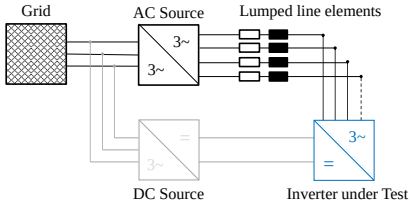

Figure 1: Laboratory environment

THE CONTROL LOOP

A generic control loop (Figure 2) consists of a controller, a controlled process and a sensor. A set point acts as the reference signal and the sensor measures the actual value of the process variable. The difference (control error) is the input to the controller, whose output is the controlled variable. The process reacts to both the controlled variable and to possible disturbances. This results in the process variable, which is measured by the sensor in return.

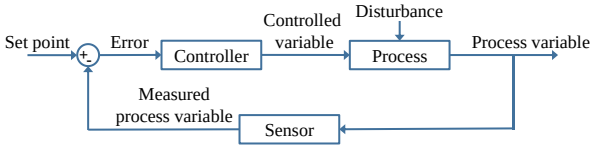

Figure 2: Generic control loop

The derived control loop

In order to derive a more descriptive architecture of the Q(V) control system, the generic form is rotated, such the grid voltage becomes the input and the reactive power the output variable of the open control loop.

$$V_{grid} = V_n + V_a - V_r = V_n + R \cdot I_a - V_r$$
$$\frac{V_r}{Q} = \frac{X}{3 \cdot V_{grid}} \approx \frac{X}{3 \cdot V_n} = K_r \quad (1)$$

Furthermore, the process block represents the connected

grid node and can be specified within the load reference system according to (1) with Ia and Ir being the active and reactive current, respectively. Phase shifting of the voltage as well as the time response of the inductivity (very small time constants) are of minor importance and can be neglected. The result in Figure 3 shows a more comprehensible form with input and output port corresponding to the measured data (V_{grid}, Q). Moreover, it is easier to implement in simulation environments by considering the open loop path only ($V_{grid} \rightarrow Q$). The sensor and controller blocks are to be identified.

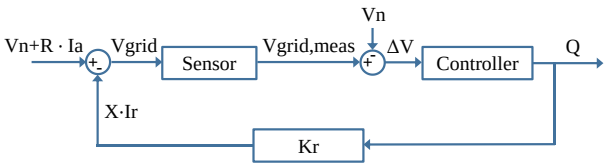

Figure 3: Derived Q(V) control loop

METHOD

Two Q(V) control-loop structures used in current commercially available inverters are modelled and evaluated based on measured data from transient events. The transient voltage events are explicitly chosen to be significant excitations to the control system. Since it covers the full frequency spectrum, an ideal step signal is the optimal excitation applied in control systems engineering [6]. Hence, various step responses of the examined inverters under varying parameterizations are recorded in laboratory grid emulations. The results are analysed, employing known methods of control engineering. The voltage step rises in 10ms from 230V to 240.32V.

Parameter variation

The considered inverters offer the parameterization of a first order transfer function (PT1) by means of a gain and a time constant as well as the implementation of a Q(V)-characteristic along 5 sampling points. It is not known where and how the elements are implemented within the control system. An ideal PT1 transfer function is shown in (2), where 's' is the complex frequency parameter and 'K' and 'T' represents for the gain and the time constant, respectively.

$$G_{PT1}(s) = \frac{K}{T \cdot s + 1} \qquad (2)$$

The implemented Q(V)-Characteristics, depicted in Figure 4, show a fixed voltage deadband of 0.03p.u. around the nominal voltage, varying gradients of reactive power per voltage and a fixed saturation value of ±4500VAr. Of notably performance is the observation, that the 1125VAr/V and the 500VAr/V slope gradients will not enter the saturation zone when applying the voltage step from 237 to 240.3 V. This implies that the characteristics can be replaced with a gain only for these cases. The adjustable parameters and their used settings can be summarised as follows:

PT1 transfer function		Q(V)-characteristic
Gain 'K'	Time constant 'T' [s]	Slope gradient [VAr/V]
1, 50	0, 1, 5, 10 s	500, 1125, 2250, 4500

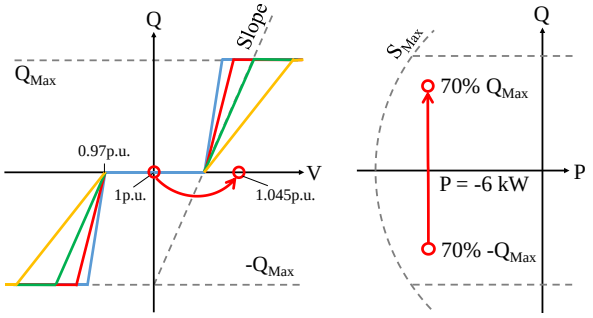

Figure 4: Q(V)-characteristic with different slope gradients (left) and PQ diagram

First estimation

A 2nd order transfer function of a system with a denominator degree n ≥ m = 2 is given according to (3):

$$G_{PT2}(s) = \frac{b_0}{a_2 \cdot s^2 + a_1 \cdot s^1 + a_0} \qquad (3)$$

Using the Laplace limit theorem, the systems general behaviour can be classified [6]. The order of the time derivative, for which the value at t=0 is not equal to zero, defines the order of the transfer function. For example, a system response to a step function is as described in (4):

$$\begin{aligned} \dot{x}_o(t \rightarrow 0) &= \lim_{s \rightarrow \infty}(s \cdot G(s) \cdot x_{i0}) = 0 \\ \ddot{x}_o(t \rightarrow 0) &= \lim_{s \rightarrow \infty}(s \cdot s \cdot G(s) \cdot x_{i0}) \neq 0 \end{aligned} \qquad (4)$$

The nonzero value of the second order time derivative indicates a second order transfer function (PT2) or any transfer function with n = m+2. In case of a nonzero value for the first order time derivative, a PT1 transfer function can be assigned (see (2)). Usually, measured data inherit signal noise due to measurement accuracies and interfering phenomena. Such data can therefore not be used to identify transfer function degrees higher than two.

Step responses with T = 0 s

When changing the PT1 time constant setting of the inverter to zero, only the hardcoded part of the open control loop and the PT1 gain operates (5), but with an altered gain. The dynamic performance following these settings can be used to identify non-alterable elements and nonlinear behaviour to a certain extent.

$$\begin{aligned} G_{open\_PT1}(s) &= \frac{b_0}{(T_{fix} \cdot s + 1)} \cdot \frac{K}{(T \cdot s + 1)} \\ &\overset{T=0}{\Longrightarrow} \frac{K \cdot b_0}{(T_{fix} \cdot s + 1)} \end{aligned} \qquad (5)$$

Step responses with extreme parameterizations

Extreme parameterizations can be used to identify some nonlinear elements, such as saturations or rate limiters by using high gains or dead time elements, as long as they are not interfering with other phenomena inside or outside of the control loop. Due to the stiff 'grid' and fixed voltage source in this investigation, most of the effects can be assigned to the open control loop.

RESULTS

INVERTER A

32 measurements have been conducted for inverter A, varying the gain 'K', the time constant 'T' and the slope gradient across the full range. The dynamic performance varied between stable and slow reactions and highly oscillating operations (Figure 5).

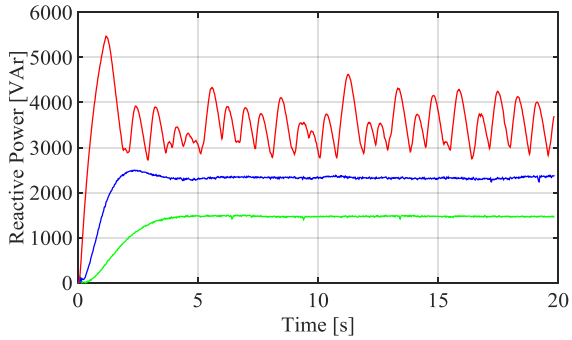

Figure 5: Step responses for K=1, T=1, 500VAr/V (green) / K=1, T=5, 1125VAr/V (blue) / K=50, T=1, 4500VAr/V (red)

Hardcoded transfer function

To avoid the appearance of nonlinear effects and to reduce the system to its hardcoded part, the measurement for the parameters K=1, T=0 and a slope gradient of 1125 VAr/V is considered. Hence, the Q(V)-characteristic can be replaced with a constant gain k_{QV}. Observing the general appearance and the first two time derivatives in Figure 5, one can classify the hardcoded part of the system as a second order transfer function.

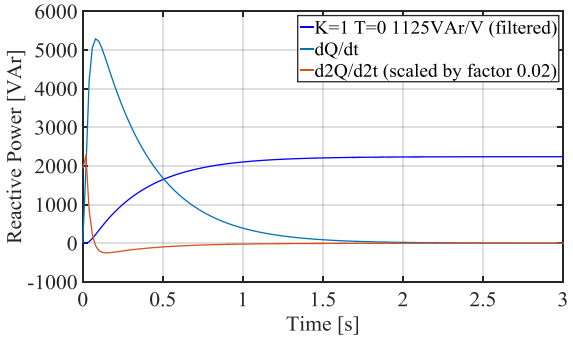

Figure 6: Step response and its time derivatives

Obviously one of the two time constants is much larger than the other, causing the step response to appear as that of a delayed PT1 element. A small delay of ≈20ms can be identified. This is usually the case, when a moving average filter, sensor or fast cascaded controller is implemented. In this case, the delay is caused by a single period RMS calculation algorithm. Neglecting the small time delay leads to only one PT1 element within the controller block and to an overall system behaviour similar to a PT1 element. Hence, it is possible to calculate a hardcoded open loop PT1 element according to (6):

$$G(s) = \frac{K_{sys}}{T_{sys} \cdot s + 1} \widehat{=} \frac{\frac{K_{QV} \cdot K_{PT1}}{1 + K_{QV} \cdot K_{PT1} \cdot K_r}}{\frac{T_{PT1}}{1 + K_{QV} \cdot K_{PT1} \cdot K_r} \cdot s + 1} \quad (6)$$

With K_{sys}=680 and T_{sys}=0.38s being read from the measured data, the PT1 time constant can be calculated as T_{PT1} = 1s, while the respective gain results in K_{PT1} = 1.5. Investigating the corresponding 500VAr/V slope gradient measurement confirms the calculated values.

Nonlinear elements

To push the system into nonlinear behaviour, high gains have to be applied. For that reason, the measurement involving K=50, T=10 and a slope gradient of 4500VAr/V is chosen for analyses (Figure 7).

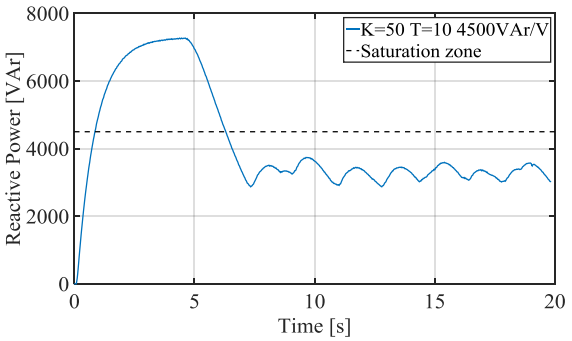

Figure 7: Nonlinear step response of inverter A

Examination of the existing measurements with high gain leads to a time constant value of T=1s for the big overshoot, confirming the previously calculated values. It is clearly visible, that the reactive power output exceeds the implemented saturation zone of ± 4500VAr. This is only possible, if the additional gain – and with it the adjustable PT1 element – is placed downstream of the Q(V) characteristic and upstream of the hardcoded PT1. Despite the high slew rate of the reactive power, it never exceeds 7500VAr, which falls in line with the inverters' cos(φ) limit. A saturation element is placed upstream of the current controller. Further calculations and processing steps lead to the mathematical description of the adjustable PT1 element shown in (7):

$$G_{PT1\_adj}(s) = \frac{0.5 + K}{0.19 \cdot s + 1} \quad (7)$$

In order to construct the complete control loop shown in Figure 13, the identified linear transfer functions and nonlinear elements have to be combined. The validation results are shown in figure Figure 8.

.

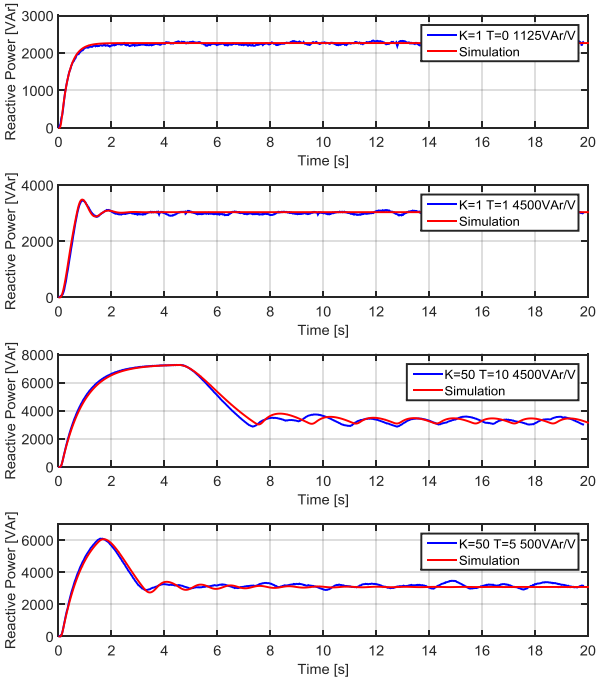

Figure 8: Validation of inverter A's model

INVERTER B

16 Measurements have been examined to identify inverter B's dynamic behaviour, leaving K fixed to 1 due to manufacturer limitations and varying T as well as the slope gradient. Throughout all measurements, inverter B shows a more stable, but also nonlinear response to step signal excitations (see Figure 9)

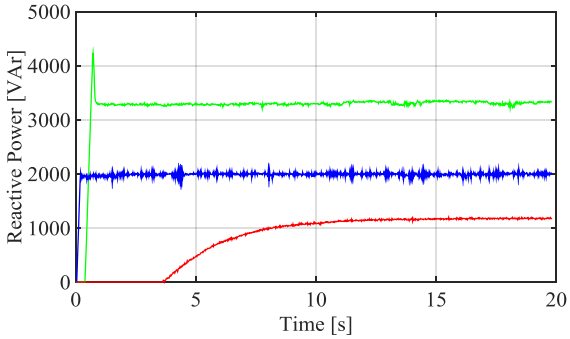

Figure 9: Step responses for K=1, T=1, 4500VAr/V (green) / K=1, T=0, 1125VAr/V (blue) / K=1, T=10, 500VAr/V (red)

Hardcoded transfer function

As before, the measured data involving a parameterization of T=0 and a slope gradient of 1125VAr/V is used to identify the hardcoded part of the control system. Figure 10 shows the corresponding step responses. The small time delay at the beginning is once again attributable to an RMS calculation algorithm downstream of the analog voltage sensor and is being represented in the final model as a PT1 element with a time constant of 0.035s.

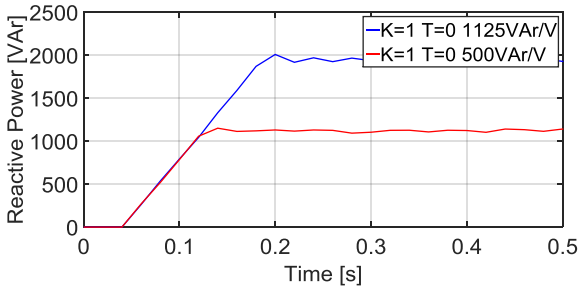

Figure 10: Step response for T=0, 1125VAr/V and 500VAr/V

The nonexistence of an exponential function in the step response using the lowest slope gradient proves, that there is no hardcoded PT1 element in the open loop, instead a rate limiter with the value of dQ/dt=13000 is present.

Adjustable PT1 element

Given the measurements for a parameterization of T=5s and 10s and a slope gradient of 500VAr/V (see Figure 11), a PT1 element upstream of the Q(V) characteristic can be assumed. A PT1 element downstream of the characteristic would delay the reactive power output, but would not create any form of dead time, ideally.

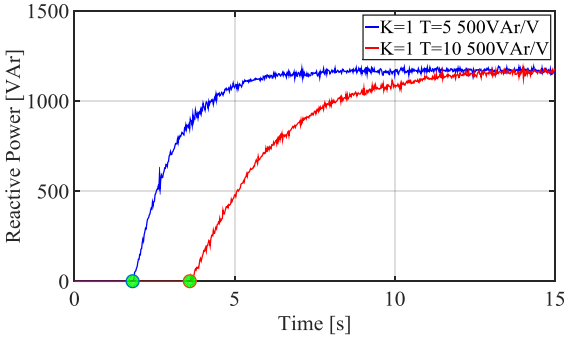

Figure 11: Step responses to identify the adjustable PT1 element

Continuing this thought leads to a PT1 element that filters the voltage input. Incorporating the known voltage step of 10.3241V (starting from 230V) and the upper dead band of 237V, one can calculate the time constant of the exponential function according to (8), where 't' is the time point marked in Figure 11.

$$V_{PT1}(t) = V_{step} \cdot \left(1 - e^{-\frac{t}{T_{PT1}}}\right) = V_{dead} - V_N$$

$$T_{PT1} = -\frac{t}{ln\left(1 - \frac{V_{dead} - V_N}{V_{step}}\right)} \quad (8)$$

The time constants calculated from all measurements show a ratio between calculated and input value of about 0.32. Including the fact, that the parameter of this inverter is called 'set-up time' and not 'delay time' one can identify the input value 'T' as the time, when ≈92.5% of the target value is reached. The validation results of inverter B's complete control loop are shown in Figure 12, whereas the control loop itself is pictured in Figure 14.

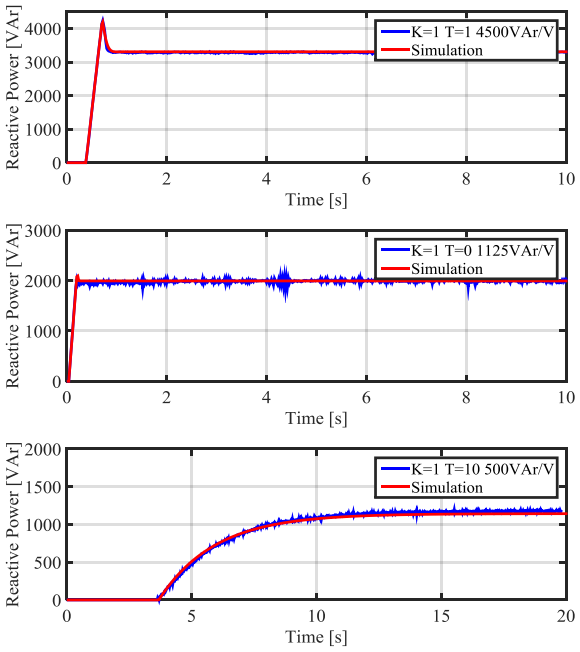

Figure 12: Validation of inverter B's model

SUMMARY

Two dynamic RMS simulation models of latest photovoltaic inverters have been constructed using measurements with varying parameter sets. The resulting models have been validated against a significant number of measurements and yield a very high consistence. Subsequently, they can be incorporated into transient simulation models to determine the stability of distribution grids with a high degree of decentralised energy resources using reactive power control. Possible instabilities, which have been shown and discussed in previous works [1,2,3,5] can be reconstructed and investigated in a more detailed way, theoretically as well as in practice. The stable operation settings acquired in [3,4] can also be confirmed. It can further be shown, that a high gain mostly leads to unwanted results, while larger time constants can both be smoothing or inducing, depending on the other parameters. The constructed models are to be used and incorporated, in order to create a better understanding of the dynamic performance of Q(V) controllers and to increase their broad acceptance in practical fields.

PROSPECTS

The linkages to theoretical stability analyses, such as the root locus and bode diagram methods as well as nonlinear stability approaches, are subject to further research. Equally considerable are the effects of low level power electronics.

AKNOWLEDGEMENT

The presented models have been developed using measurements obtained within the project "Statische Spannungshaltung" funded by the VDE forum of Network Technology / Network Operation (FNN) in Germany.

REFERENCES

[1] D. Schacht, et al., 2013, "Planungsgrundsätze für den effizienten Einsatz und die Umsetzung einer Spannungsregelung durch Erzeugungsanlagen in Verteilungsnetzen." ETG-Kongress/VDE VERLAG

[2] F. Andrén, et al. "On the Stability of local Voltage Control in Distribution Networks with a High Penetration of Inverter-Based Generation." (2014)

[3] FNN/VDE, „Vergleich von technischer Wirksamkeit sowie Wirtschaftlichkeit zeitnah verfügbarer Verfahren zur Sicherung der statischen Spannungshaltung in Niederspannungsnetzen mit starker dezentraler Einspeisung"

[4] P. Esslinger, R. Witzmann, 2012, "Studie Q(U)." Technische Universität München.

[5] H. Basse, et al., 2009, "Dynamische Auswirkungen einer spannungsabhängigen Blindleistungsregelung bei dezentralen Einspeisern." ETG-Kongress/VDE VERLAG

[6] H. Lutz, W. Wendt, 2007, „Taschenbuch der Regelungstechnik", Harri Deutsch Verlag

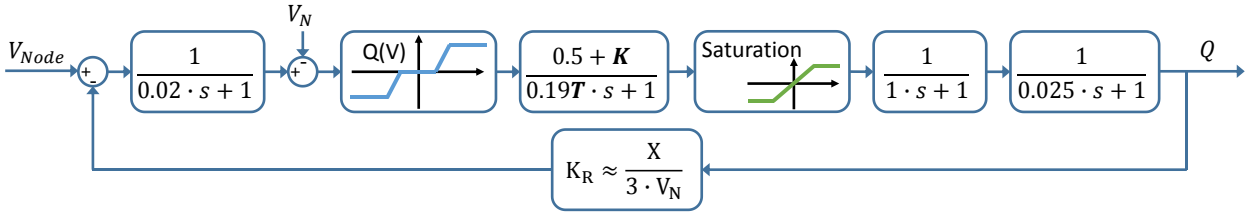

Figure 13: Complete control loop model of inverter A

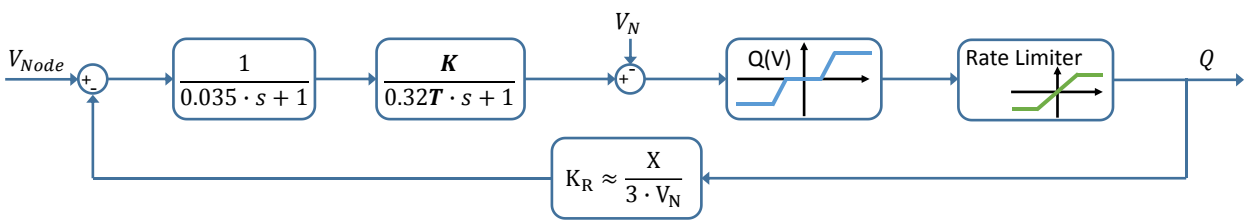

Figure 14: Complete control loop model of inverter B